# 2022 WUOF/SIU International Consultation on Urological Diseases: Imaging of Renal Cell Carcinoma

Wai-Kit Lee,[1] M. Liza Lindenberg,[2] Esther Mena Gonzalez,[2] Peter Choyke,[2] Kevin G. King,[3] Raghunandan Vikram,[4] Vinay A. Duddalwar[5]

[1]Department of Medical Imaging, St. Vincent's Health, University of Melbourne, Fitzroy, Australia [2]Molecular Imaging Branch, Center for Cancer Research, National Cancer Institute, NIH, Bethesda, United States [3]Keck School of Medicine of USC, University of Southern California, Los Angeles, United States [4]Department of Abdominal Imaging, Division of Diagnostic Imaging, The University of Texas MD Anderson Cancer Center, Houston, United States [5]Keck School of Medicine of USC and USC Viterbi School of Engineering, University of Southern California, Los Angeles, United States

## Abstract

Imaging plays a central role in the contemporary multidisciplinary management of renal cell carcinoma. This article provides an overview of the current imaging modalities, including ultrasound, computed tomography, multiparametric magnetic resonance imaging, and molecular imaging, used in the evaluation of renal cell carcinoma. A summary of the imaging strategies for renal cell carcinoma staging and restaging post-treatment is provided.

## Introduction

Imaging allows for the detection, characterization, staging, treatment planning and guidance, post-treatment evaluation, and surveillance of renal cell carcinoma (RCC). An understanding of the advantages and limitations of each imaging modality, and the evolving role of imaging in newer management strategies (such as active surveillance, ablation, and embolization) and the utility of newer therapeutics (such as antiangiogenic treatments and immunotherapy) is critical. The purpose of this narrative review is to provide an overview of the current imaging modalities, such as ultrasound (US), multidetector computed tomography (CT), multiparametric magnetic resonance imaging (MRI), and molecular imaging, used in the evaluation of RCC; highlight newer imaging techniques, such as contrast-enhanced US (CEUS) and novel molecular imaging agents, as well as radiomics with artificial intelligence technology; and provide a summary of the imaging strategies for RCC staging and post-treatment restaging. Imaging findings following newer treatment techniques, such as ablation and systemic therapy for advanced RCC, are beyond the scope of this article.

## Detection and Diagnosis

Clear cell renal cell carcinoma (ccRCC) (70%–80%), papillary renal cell carcinoma (pRCC) (10%–15%), and chromophobe renal cell carcinoma (chRCC) (5%) are the 3 most common histologic subtypes of RCC[1], which as a group show a broad spectrum of imaging appearances. Multiphase contrast-enhanced CT is the imaging modality most commonly used for the evaluation of RCC[2]. A systematic review found that the median sensitivity and specificity of CT for the diagnosis of RCC were 88% and 75%, respectively[3]. A limitation of CT is the necessity for intravenous contrast agent, which may be contraindicated owing to renal dysfunction or iodine allergy.

### Key Words

Renal cell carcinoma, ultrasound, computed tomography, magnetic resonance imaging, positron emission tomography

### Competing Interests

None declared.

### Article Information

Received on July 15, 2022
Accepted on August 31, 2022
This article has been peer reviewed.

Soc Int Urol J. 2022;3(6):407–423

DOI: 10.48083/SDMV1045

## Abbreviations

AML angiomyolipoma
AUA American Urological Association
CAIX carbonic anhydrase IX
ccRCC clear cell renal cell carcinoma
CEUS contrast-enhanced US
chRCC chromophobe renal cell carcinoma
CT computed tomography
FDG 18F-fluorodeoxyglucose
MRI magnetic resonance imaging
PET/CT positron emission tomography/computed tomography
pRCC papillary renal cell carcinoma
PSMA prostate-specific membrane antigen
RCC renal cell carcinoma
SUVmax maximum standardized uptake value
US ultrasound

Multiparametric MRI is frequently used to further characterize renal masses that are indeterminate on CT, but can be used as the initial study for the evaluation of renal masses, especially in patients with contraindication to iodinated contrast material[2]. A systematic review showed that the median sensitivity and specificity of MR for the diagnosis of RCC were 87.5% and 89%, respectively[3]. A limitation of MRI is the contraindication of intravenous contrast in advanced renal disease owing to potential for nephrogenic systemic fibrosis.

Conventional US can be utilized to triage an indeterminate renal lesion incidentally detected at single-phase CT to determine whether it is a simple or minimally complex cyst or a solid lesion. A systematic review showed that the sensitivity and specificity of conventional US for the diagnosis of RCC were 46% and 12%, respectively[3]. Limitations of conventional US include its reduced sensitivity for the detection of small renal masses and the inability to further characterize solid renal masses. CEUS is superior to CT and MRI for the evaluation of septa and mural enhancement in complex cystic renal lesions[4,5] (**Figure 1**), and its median sensitivity and specificity for the diagnosis of RCC in these lesions were reported to be 94.5% and 69%, respectively[3]. However, there is no current role for CEUS in the Bosniak classification scheme, but proposals for an adaptation of the scheme incorporating CEUS features have been suggested[6]. Suboptimal image acquisition owing to patient factors, such as obesity, inability to breath-hold, and acoustic shadowing from bowel gas or ribs, can limit the utility of CEUS.

18F-fluorodeoxyglucose (FDG) positron emission tomography/computed tomography (PET/CT) is not recommended by major societies, including the American Urology Association (AUA), European Association of Urology (EAU), and National Comprehensive Cancer Network (NCCN), for the routine diagnosis or evaluation of RCC because the technique is limited by the physiologic excretion of radiotracer through the kidneys and the baseline FDG uptake in normal renal parenchyma, which can obscure part or all of the renal tumor[7–9]. Systematic reviews found that FDG PET/CT for RCC detection showed high specificity but variable sensitivity depending on the size, subtype, and grade of RCC[3,10].

## Imaging Features of Common Subtypes of RCC

### Clear Cell Renal Cell Carcinom

At US, ccRCC has variable appearances. It typically appears as a heterogeneously hypoechoic or isoechoic mass (**Figure 2**), but may show hyperechoic components[11,12]. Fluid components may be present due to cystic, necrotic, or hemorrhagic change. Doppler flow is readily identified owing to its hypervascular nature. At CEUS, ccRCC shows avid, early enhancement, followed by washout[13] (**Figure 3**). At CT and MRI, ccRCC is typically exophytic and shows vivid early contrast enhancement[14]. It has low-to-intermediate T1 signal and high T2 signal compared to adjacent renal parenchyma[15]. Internal tumor heterogeneity can occur owing to areas of hemorrhage, necrosis, and/or cystic degeneration, which appear as nonenhancing regions[16]. ccRCC may show reduced signal on opposed-phase chemical shift MR images compared to in-phase images owing to intracellular fat[17]. A peritumoral pseudocapsule may be present, which appears as a regular low or high attenuation rim on CT[18], and low T1 and T2 signal on MR images[19]. Calcifications are uncommon[20] (**Figures 4 and 5**).

### Papillary Renal Cell Carcinoma

At US, pRCC may appear as a solid, well-circumscribed mass (**Figure 6**), or sometimes may be partially solid with cystic or hemorrhagic components[11]. At CEUS, it shows hypoenhancement with a later and lower peak of enhancement compared to ccRCC[13] (**Figure 7**). At CT and MRI, pRCC is generally a small peripheral homogeneous mass that has low T2 signal compared to renal cortex, and shows weak enhancement that progressively increases on subsequent phases[21]. pRCC may show loss of signal on in-phase images compared to opposed phase at chemical shift MRI owing to hemosiderin[22]. Some pRCCs appear as hemorrhagic cystic masses with enhancing papillary projections[23]. Calcifications occur in 7% of cases[21] (**Figures 8 and 9**). Type 1 and 2 pRCCs cannot be reliably differentiated on imaging, but type 2 pRCCs are more likely to be heterogeneous, show infiltrative margins, and contain calcifications[24].

**FIGURE 1.**

Superior ability of CEUS to demonstrate septal enhancement

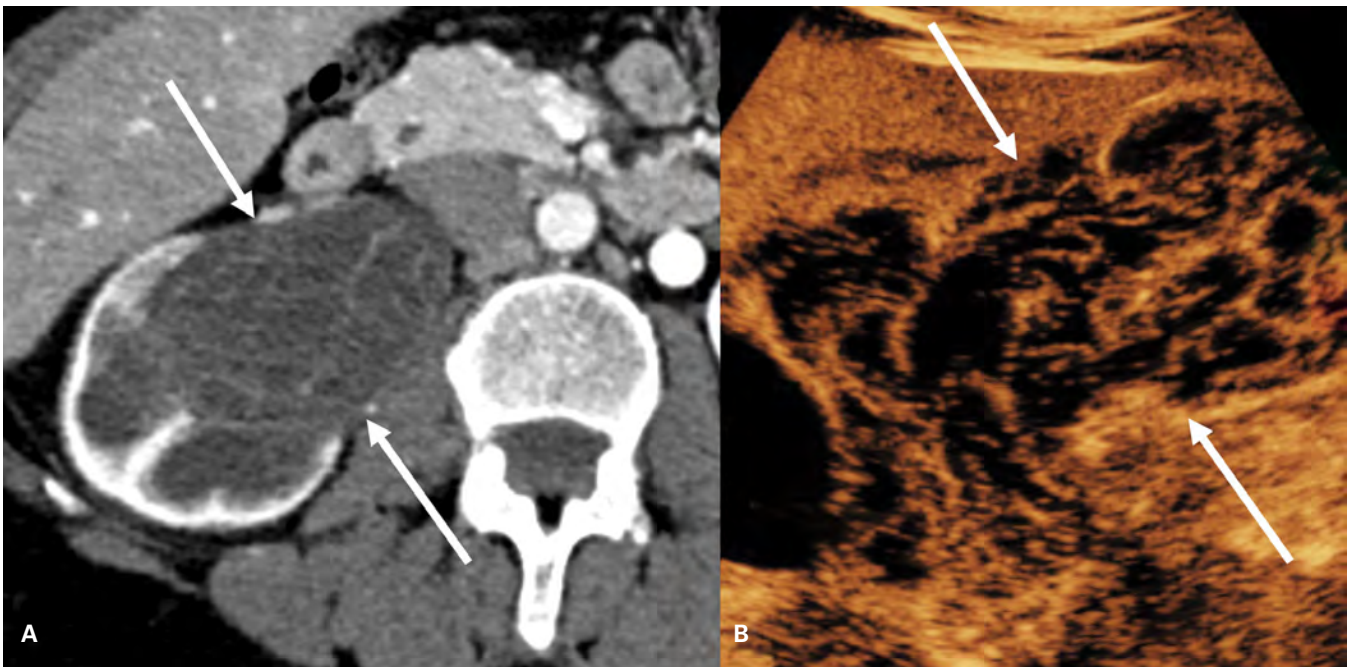


Contrast-enhanced CT (A) shows a large cystic lesion (arrows) centrally in the right kidney with several internal enhancing septations. CEUS (B) shows an even greater number of internal enhancing septations, and with superior detail. Postsurgical pathological evaluation confirmed a mixed epithelial and stromal tumor.

**FIGURE 2.**

Clear cell renal cell carcinoma

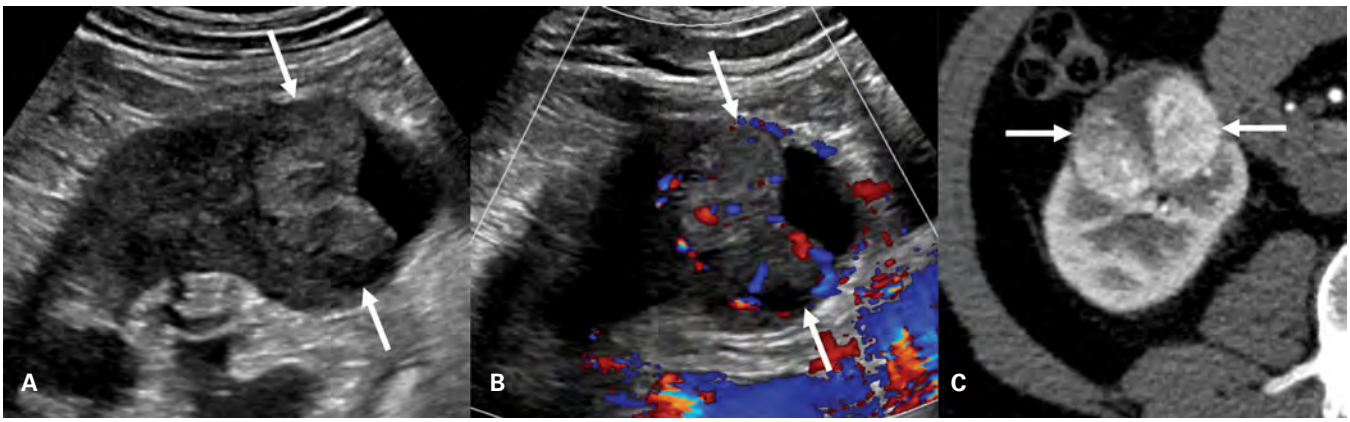


Greyscale ultrasound (A) shows a heterogeneous mass (arrows) with solid and cystic components, and color Doppler ultrasound (B) shows flow in the solid portion. Contrast-enha eterogeneous mass with avid enhancement.

## Chromophobe Renal Cell Carcinoma

At imaging, chRCC is typically a solid, well-circumscribed mass that is more homogeneous than ccRCC. At CEUS, its enhancement is often nearly isoenhancing to renal cortex and can be difficult to discriminate from ccRCC, especially with small tumors[13]. chRCC shows heterogeneous T2 signal on MRI[25]. At CT and MRI, it shows intermediate contrast enhancement in between that of ccRCC and pRCC[14,23]. A central scar, spoke-wheel enhancement pattern and segmental enhancement inversion may be present, but these features overlap with oncocytoma[25–27]. Calcifications occur in 14% to 38% of cases, and perinephric infiltration and venous invasion are uncommon[20,26].

**FIGURE 3.**

Clear cell renal cell carcinoma at CEUS

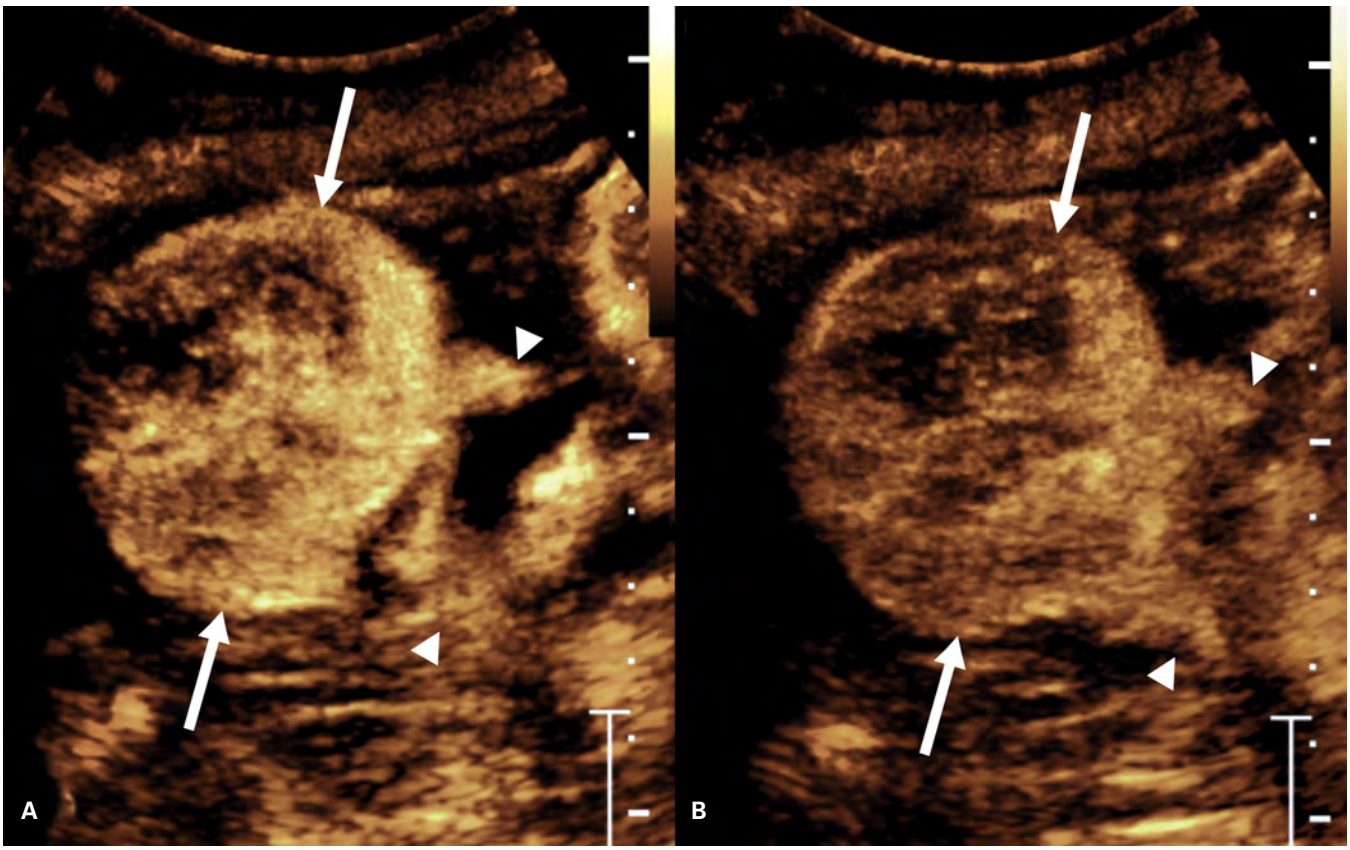


Corticomedullary phase (A) shows a heterogeneously hyperenhancing (relative to renal cortex) mass (arrows) exophytic from the right kidney (arrowheads). At delayed phase (B), the mass shows washout.

**FIGURE 4.**

Sixty-year-old male patient with typical features of clear cell renal cell carcinoma on CT

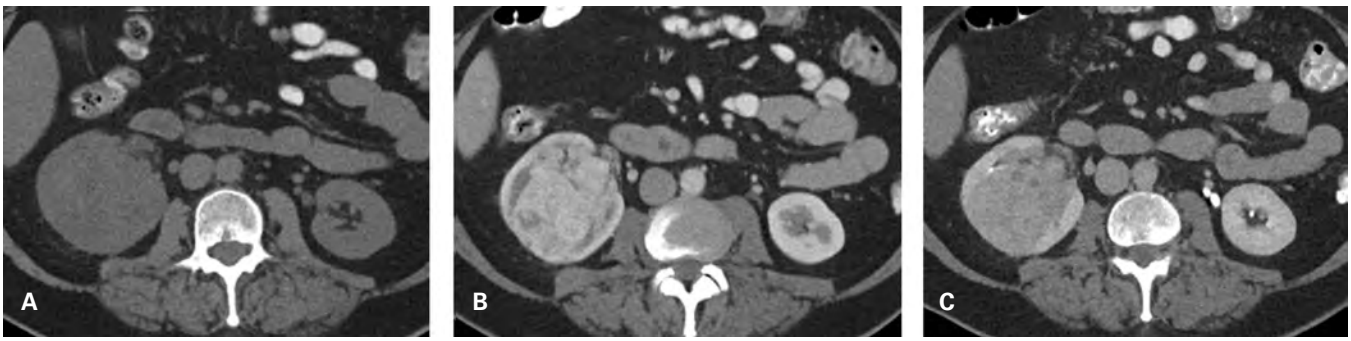


Axial unenhanced CT scan (A) shows an expansile mass involving the right kidney. Postcontrast axial CT in corticomedullary phase (B) shows heterogeneous and intense enhancement of the mass. Delayed-phase image (90 seconds) (C) shows contrast washout in the mass. This pattern of enhancement and contrast washout is typical of clear cell renal cell carcinoma.

**FIGURE 5.**

Sixty-year-old male patient with typical features of clear cell renal cell carcinoma on MRI

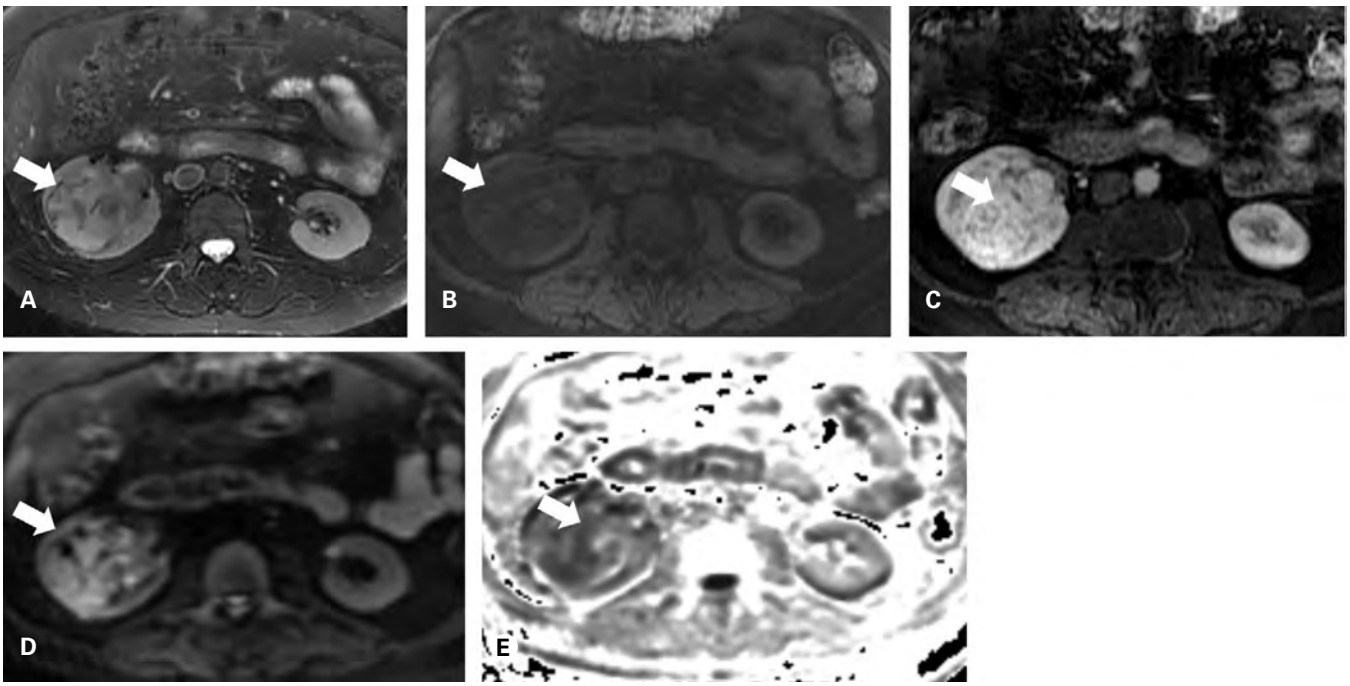


Axial T2-weighted image (A) shows a right renal mass with heterogeneous high signal. Precontrast fat-suppressed T1-weighted image (B) shows a hypointense expansile central mass. Postcontrast T1-weighted image in corticomedullary phase (C) shows intense and heterogeneous enhancement of the mass. Diffusion-weighted image (b = 500) (D) and corresponding ADC map (E) show restricted diffusion in the mass.

**FIGURE 6.**

Papillary renal cell carcinoma

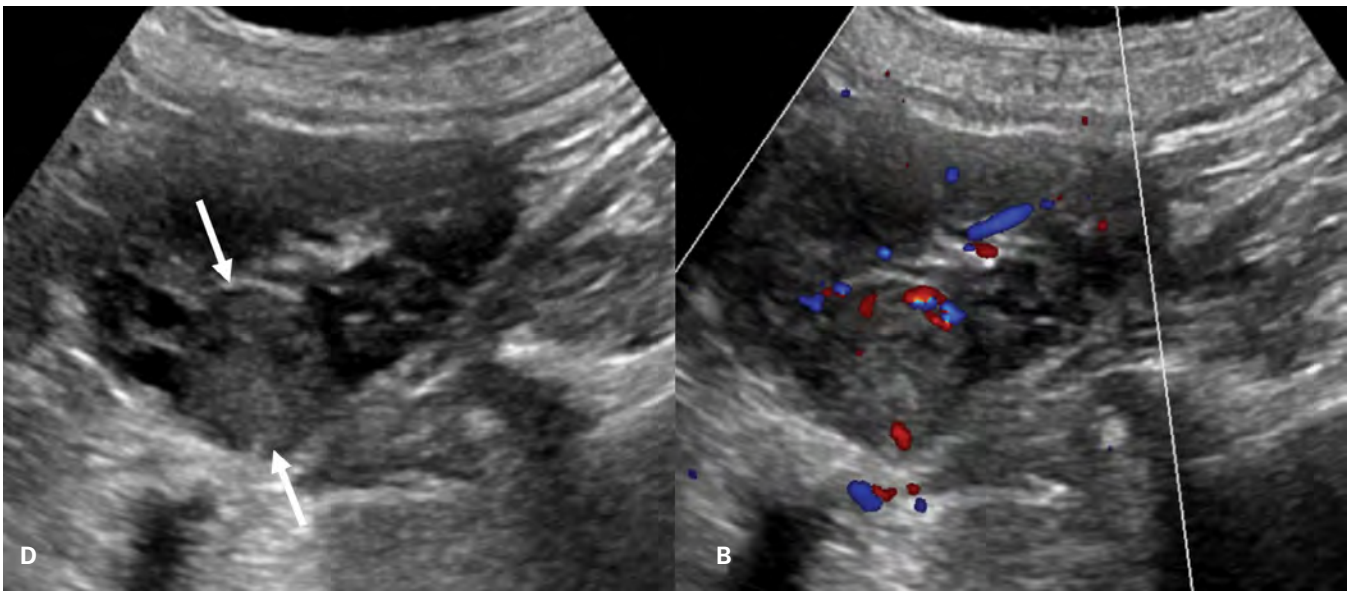


Greyscale ultrasound (A) shows a small solid, well-circumscribed mass (arrows) that is isoechoic to mildly hyperechoic, and color Doppler ultrasound (B) shows internal flow.

**FIGURE 7.**

Papillary renal cell carcinoma at CEUS

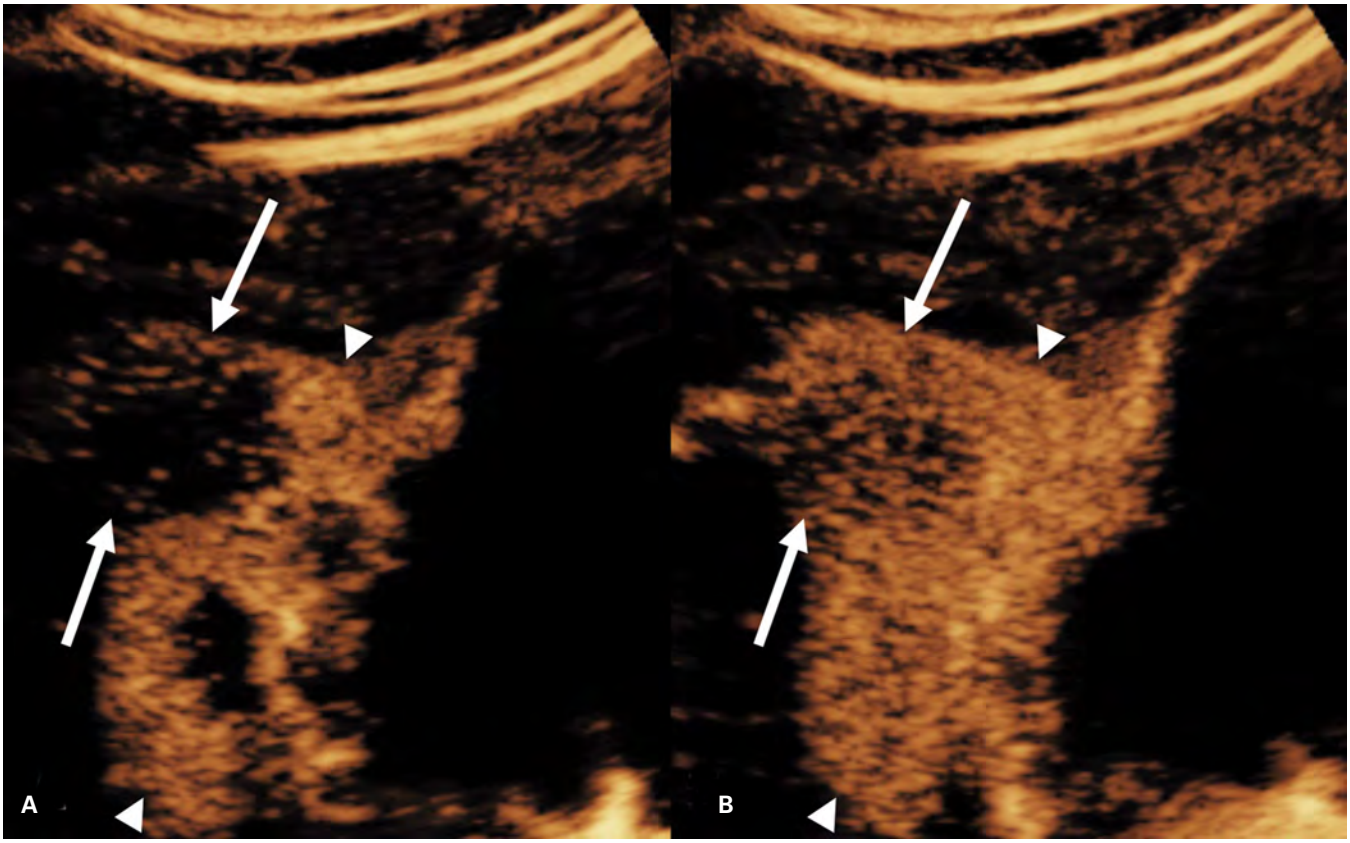


Corticomedullary phase (A) shows only slight early enhancement of the mass (arrows), much less than adjacent cortex (arrowheads). The peak of enhancement is later, at nephrographic phase (B), but even at its peak, the mass is still slightly hypoenhancing (arrows) relative to the adjacent cortex (arrowheads).

**FIGURE 8.**

Fifty-year-old male patient with an asymptomatic papillary renal cell carcinoma on CT


Axial unenhanced (A), corticomedullary phase (B), and nephrographic phase (C) CT images show an expansile mass in the upper pole of the right kidney with low-grade enhancement. This appearance is commonly seen in type 1 papillary renal cell carcinoma.

**FIGURE 9.**

Fifty-year-old male patient with an asymptomatic papillary renal cell carcinoma on MRI

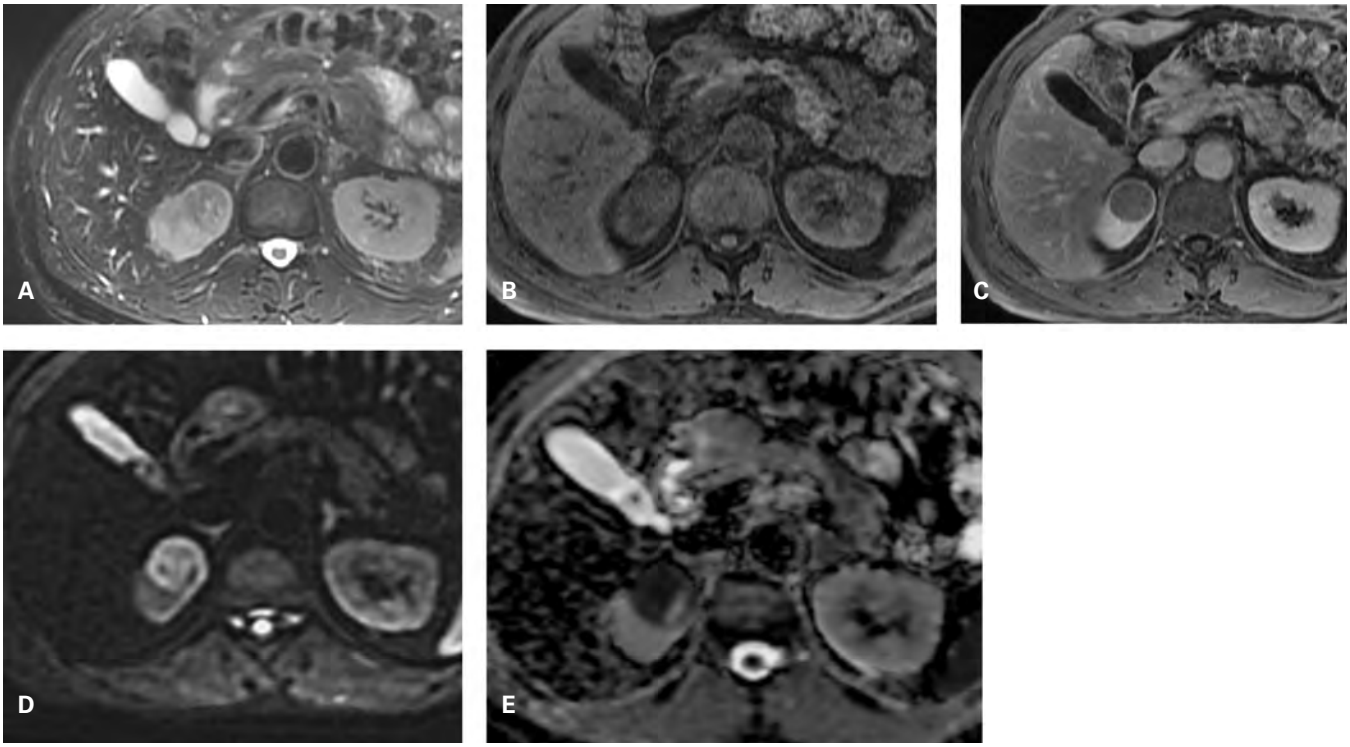


Axial T2-weighted image (A) shows an expansile partially exophytic mass in the upper pole of the right kidney with relative low signal compared to the renal cortex. Axial precontrast fat-suppressed T1-weighted image (B) and postcontrast fat-suppressed T1-weighted image in nephrographic phase (C) show relative hypoenhancement of the mass, compatible with papillary renal cell carcinoma. Diffusion-weighted image (b = 500) (D) and corresponding ADC map (E) show restricted diffusion in the mass.

## Differentiation of RCC from Benign Renal Tumors

Imaging is unable to reliably discriminate between benign and malignant renal masses owing to overlapping imaging characteristics in 10% to 15% of cases[28]. RCC can be challenging to differentiate from oncocytoma and lipid-poor angiomyolipoma (AML). However, composite imaging features can suggest a likely diagnosis. AML is a typically homogeneous and markedly hyperechoic mass on US, but up to 30% of small RCCs may be hyperechoic, and a definitive diagnosis of AML cannot be established on US appearances alone[12]. At CEUS, AML typically shows homogeneous hypoenhancement relative to renal parenchyma and can be difficult to distinguish from pRCC and chRCC[12,13]. Macroscopic fat within a noncalcified renal mass on CT is almost diagnostic of an AML. Macroscopic fat rarely occurs in RCC[29]. Intracellular fat can be identified in clear cell RCC but this feature in isolation does not allow its differentiation from lipid-poor AML[30]. A renal mass containing fat with calcification or one that shows necrosis is more likely to be an RCC than AML[23,29].

pRCC can be differentiated from a hemorrhagic cyst and lipid-poor AML because it shows weak progressive contrast enhancement. Hemorrhagic cyst shows no contrast enhancement[31], and lipid-poor AML shows avid early contrast enhancement with subsequent contrast washout[32].

chRCC and oncocytoma show multiple overlapping imaging features and are most challenging to differentiate from each other[25,33]. At CEUS, oncocytoma typically shows hyperenhancement and can show persistent delayed enhancement, but the features are inadequate to allow for confident discrimination from chRCC[12]. Quantitative imaging parameters, such as tumor enhancement characteristics[34,35], diffusion-weighted MRI[36], and texture analysis[37], have shown some ability to differentiate between benign and malignant renal masses.

## Differentiation of Subtypes of RCC

Imaging is as of yet unable to reliably differentiate between the subtypes of RCC owing to overlapping imaging characteristics. A study showed the performance of CT to predict ccRCC and chRCC on morphologic features alone had a positive predictive value of less than 75%, but evaluation of their contrast

enhancement profile allowed for differentiation of ccRCC from other subtypes with a sensitivity, specificity, and accuracy of 64%, 87%, and 75%, respectively[34]. Dynamic contrast-enhanced MRI studies found that RCC subtypes showed contrast enhancement profiles concordant with CT findings, but considerable overlap occurs and does not allow for definitive tumor histologic subtyping[14,35]. The application of algorithmic and scoring systems, such as the clear cell likelihood score, would help to achieve greater accuracy[38,39]. Type 1 and 2 pRCCs show overlapping imaging findings that do not permit reliable differentiation between them on morphological features[14,24] or metabolic parameters[40,41]. Early dynamic imaging with FDG PET/CT may be more helpful than traditional static scanning in distinguishing aggressive RCC subtypes. A study showed that the maximum standardized uptake value (SUVmax) from dynamic scans was higher in ccRCC than non-ccRCC[42]. Another study showed that chRCC demonstrated lower SUVmax values than ccRCC and pRCC, but there was no significant difference between ccRCC and pRCC[43].

### Grading of RCC

Nuclear grade of RCC correlates with patient survival[44]. Imaging features that act as accurate surrogate markers of histologic grade of RCC would allow for noninvasive prediction of prognosis and triage management. Most studies have attempted to differentiate between low- and high-Fuhrman grade ccRCC. One study showed that the sensitivity and specificity of MRI to diagnose low-grade ccRCC were 50% and 94%, respectively, and to diagnose high-grade ccRCC they were 93% and 75%, respectively[45]. Another study showed no significant correlation between histologic grade and MRI features for pRCC and chRCC[46]. Morphologic imaging features suggestive of higher grade tumor or sarcomatoid dedifferentiation include larger tumors with intratumoral necrosis, calcification, infiltrative margins, increased peritumoral neovascularity, larger peritumoral vessels, and renal vein thrombosis[45,47–48]. An uncommon predominantly cystic appearance of ccRCC has been shown to have low-grade malignant potential[49]. FDG PET/CT studies showed that higher SUVmax and tumor-to-normal reference tissue ratios corresponded to more aggressive RCC features, such as higher TNM stage and Fuhrman grade, as well as presence of venous and lymphatic invasion[42,43]. One FDG PET/CT study showed higher maximum, mean, and peak standardized uptake values in RCC with sarcomatoid differentiation compared to ccRCC[50]. Other metabolic measures, such as metabolic tumor volume and tumor-to-liver ratios, also appear to correlate with RCC grade[51,52]. Quantitative imaging parameters, such as tumor enhancement characteristics[53], diffusion-weighted MR imaging[54], and texture analysis[55,56], have shown some correlation with nuclear grading.

## Staging

The 8th edition of American Joint Committee on Cancer TNM staging manual is the most commonly used staging system for RCC[57] (**Table 1**). The American College of Radiology appropriateness criteria recommend CT or MRI of the abdomen without and with contrast as the most appropriate imaging modalities to stage RCC[58]. CT and MRI have similar accuracy for the staging of the primary tumor[59,60]. However, CT is more commonly utilized owing to its ready availability and rapid acquisition time. MRI is generally utilized when iodinated contrast medium administration is contraindicated. US is generally considered inferior to CT or MRI in staging and post-treatment evaluation for RCC, but it has a role in select patients. CEUS can be helpful in certain situations if CT/MRI remains indeterminate, or if CT/MRI cannot be performed with contrast (**Figure 10**). CT chest is recommended at initial staging, as the lungs are the most common site of RCC metastases[8,61]. Targeted imaging should be considered in patients with organ-specific symptoms, such as MRI or CT of the brain in patients with neurological symptoms, or bone scintigraphy in patients with bone pain, elevated alkaline phosphatase, or radiographic findings suggestive of bone metastases[61]. Bone metastases from RCC are typically lytic, and the poor osteoblastic response may limit the uptake of radiotracer at bone scintigraphy. One study of patients with stage IV RCC showed that the sensitivity of bone scintigraphy for the detection of osseous metastases was 29%[62].

### Evaluation of Primary Tumor

Key imaging features of the primary tumor to be evaluated include the tumor's size, location, degree of local invasion (into collecting system, perirenal fat, perirenal fascia, and adjacent organs), and renal vascular anatomy[63]. However, both CT and MRI may underestimate tumor size, as well as early urinary collecting system, renal sinus fat, and perinephric fat invasion, compared to pathologic examination, which may result in tumor upstaging[64–67].

### Evaluation of Nodes and Distant Metastases

The most common sites of RCC metastases, in descending order of frequency, are the lungs, bones, liver, lymph nodes, adrenal glands, and brain[68,69]. However, metastases to any organ can occur. Cross-sectional imaging criteria for the diagnosis of metastatic lymph nodes rely on size larger than 1 cm in short-axis diameter, abnormal shape, disruption of the normal lymph node architecture, and abnormal contrast enhancement characteristics mirroring those of the primary tumor[70]. The accuracy of CT and MRI for

**TABLE 1.**

T staging categories

| | |
|---|---|
| Tx | Primary tumor cannot be assessed |
| T1 | T1a: ≤ 4 cm, limited to the kidney<br>T1b: > 4 cm and ≤ 7 cm, limited to the kidney |
| T2 | T2a: > 7 cm and ≤ 10 cm, limited to the kidney<br>T2b: > 10 cm, limited to the kidney |
| T3 | T3a: invades renal vein/branches, perirenal fat, renal sinus fat, or pelvicalyceal system<br>T3b: extends into vena cava below the diaphragm<br>T3c: extends into vena cava above the diaphragm or invades vena cava wall |
| T4 | Invades beyond Gerota's fascia, including direct extension to adrenal gland |

*Amin MB and Edge SB. AJCC Cancer Staging Manual, 8th Edition. Springer Nature Switzerland AG; 2017*[57]

lymph node staging is 83% to 88%[69]. Both CT and MRI are unable to differentiate enlarged, reactive nodes from metastatic lymph nodes or identify micrometastases in normal-sized lymph nodes[69,71]. A review showed that FDG PET had a sensitivity and specificity of 75% and 100%, respectively, for the detection of lymph node metastases in RCC[71] (**Figure 11**).

## Imaging in Follow-Up

In RCC, 80% to 85% of tumor recurrence occurs within the first 3 years following surgery[69,72]. The incidence of local recurrence at the surgical bed following surgery for localized RCC is about 2%[69]. Risk for tumor recurrence following surgery depends on the pathological size, stage, grade, and histologic subtype of the primary tumor[69]. Pathological stage and grade of the primary tumor enable risk stratification of surgical candidates[57,61]. Patients with positive surgical margin are considered to be in at least one higher level of risk category than that based upon their surgical specimen[61].

There is no consensus on the surveillance program following treatment. A risk-based postoperative surveillance schedule has been recommended by the AUA[61] as well as EAU[8]. Contrast-enhanced CT or MRI of the abdomen as well as chest imaging are suggested with each follow-up visit[61]. Chest radiograph is

**FIGURE 10.**

Renal vein tumor invasion on CEUS

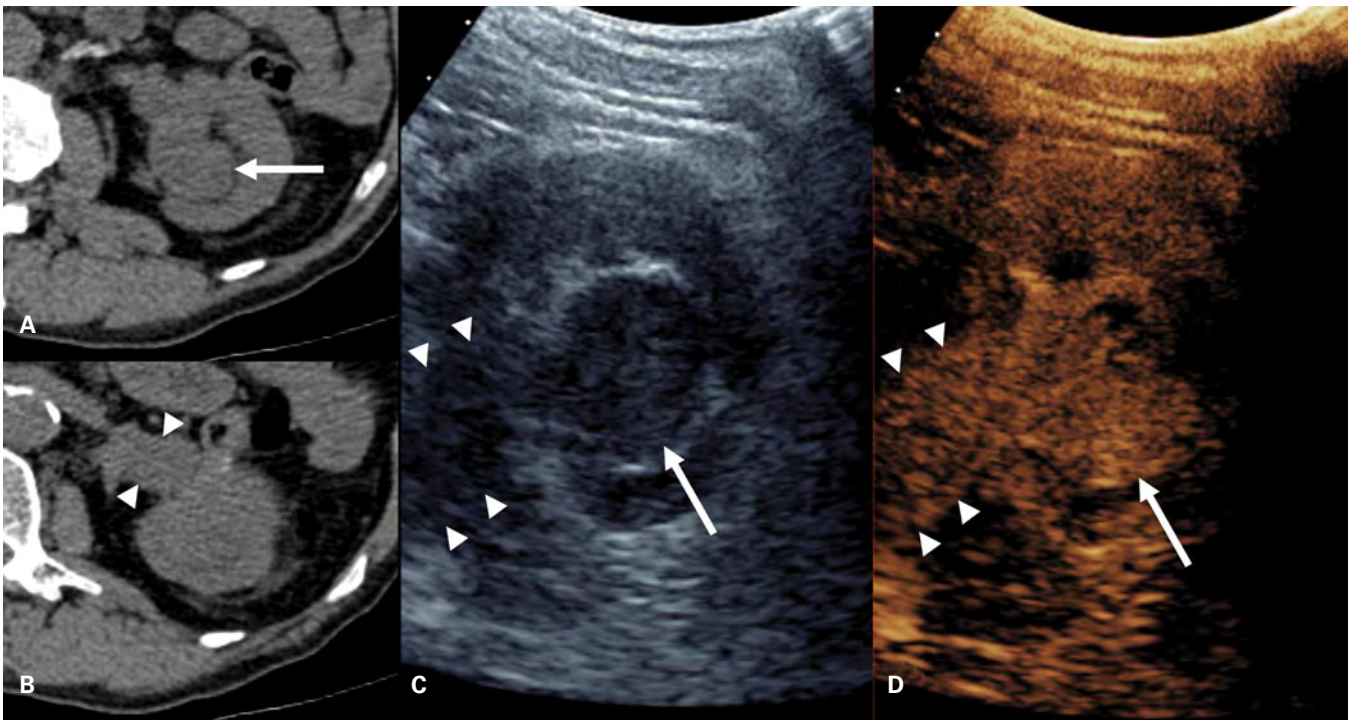


Noncontrast CT (A) shows a left renal lower pole mass (arrow), and a more cranial image (B) shows expansion of the renal vein (arrowheads), concerning for tumor invasion or bland thrombus. Greyscale US (C) shows the mass (arrow) and the renal vein (arrowheads) to have similar echogenicity. CEUS (D) shows tumor enhancement (arrow) that is contiguous with enhancing tissue in the renal vein (arrowheads), confirming venous invasion by tumor.

**FIGURE 11.**

Papillary renal cell carcinoma metastases on PET/CT

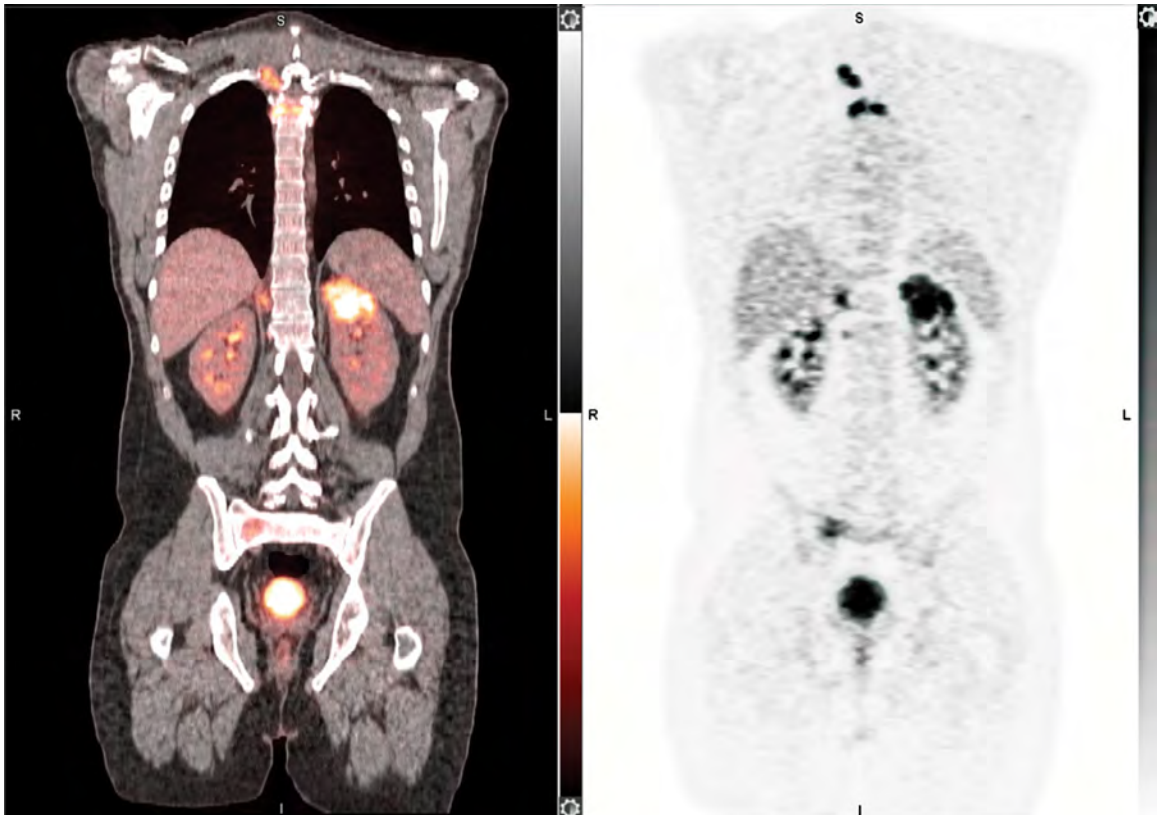


18F-FDG PET/CT shows focal uptake in the primary left upper pole papillary renal cell carcinoma and in metastatic lesions in the ribs, spine, pelvis, and retrocrural lymph nodes. Physiologic activity is within the renal collecting system and bladder. Coronal PET and CT fusion image is on the left, and coronal PET is on the right.

recommended for those in low-risk and intermediate-risk categories, and chest CT is recommended for those in high-risk and very high-risk categories[61]. US alternating with CT or MRI may be considered in low-risk and intermediate-risk groups after the initial 2 years of follow-up after surgery or ablation, and in active surveillance of localized renal masses[61]. Patients managed with ablative treatments are recommended to follow an intermediate-risk category surveillance schedule[61]. Patients with relapse, stage IV disease, and surgically unresectable disease are recommended to undergo CT or MRI every 6 to 16 weeks at the physician's discretion and patient's clinical status[9].

A detailed discussion of the imaging manifestations following ablation and systemic therapy with targeted agents, such as antiangiogenic agents and immunotherapy, is beyond the scope of this article. Traditional evaluation of tumor size to determine therapy response may be inadequate in these settings. Imaging findings supportive of favorable response include development of marked necrosis, decrease in tumor attenuation, and change in pattern of enhancement[73].

Currently, AUA recommends that PET/CT should not be routinely obtained but may be considered in select cases[61]. A meta-analysis showed that the pooled sensitivity and specificity were 86% and 88%, respectively, of 18F-FDG PET/CT for the detection of metastatic disease in RCC[74]. Another study showed that PET/CT was comparable to CT for the detection of metastatic disease after surgery[75]. PET/CT may have prognostic benefit and can influence clinical decision. A study showed that positive PET/CT scan correlated with lower progression-free survival at 3 years and lower overall survival by 5 years, which affected management decision in 43% of patients[76]. Another study showed that the high number of FDG-positive RCC metastases or metastases with high SUVmax at baseline PET/CT were linked to shorter overall survival[77]. Furthermore, the study showed that disease progression on PET/CT at 16 weeks after start of treatment correlated with decreased overall survival and progression-free survival. Qualitative metrics, such as total lesion glycolysis and metabolic tumor volume, were also shown to be predictive of overall survival and progression-free survival[78,79].

A summary of the currently recommended imaging modalities to be utilized according to the stage of the disease is included (Table 2).

## Imaging-Assisted Interventions

Renal mass biopsy, percutaneous tumor ablation, and intraoperative surgery can be assisted by real-time imaging. Image-guided percutaneous renal mass biopsy has become more commonly performed and can be guided by US or CT. Biopsy may help to avoid surgery by demonstrating benign pathology, or if showing malignancy can help guide management decision to surgery, ablation, or active surveillance. Image-guided percutaneous thermal ablation of a renal mass is an alternative to surgery in select patients with localized tumors and can be potentially curative. Intraoperative US can be utilized as an adjunct to assist surgery by increasing confidence in selection of the site of parenchymal transection, aid in evaluation of the relationship of the mass to renal vessels and renal collecting system, verify extent of inferior vena caval tumor, and aid in detection of additional lesions[80,81]. Three-dimensional (3D) imaging technology, such as 3D printing model, augmented reality, and mixed reality technology, is a novel application of CT or MR imaging dataset to produce a visually concise representation of a renal tumor to improve its localization within the kidney and understand its relationship to relevant anatomical structures. Three-dimensional printing models and augmented reality have been utilized for preoperative surgical planning in complex cases[82] and for patient counseling[83].

## Future Directions

A number of novel imaging techniques are being investigated to further characterize indeterminate renal masses including elastography, dual-energy spectral CT and perfusion CT, novel PET radiotracers, 99m Technetium sestamibi, and the utility of radiomics with artificial intelligence[84,85].

Advanced US techniques, such as elastography, are being studied for their potential to differentiate between benign and malignant renal masses[86]. Advanced CT techniques, such as dual-energy spectral CT and perfusion CT, are being studied but their exact role in renal mass CT protocol is unclear. Studies have shown mixed results in the ability of dual-energy spectral CT and perfusion CT to differentiate between benign and malignant renal masses[87], RCC subtypes[88], and RCC histologic grade[89]. The higher radiation dose penalty and more challenging technique of perfusion CT may limit the technique's wider utility in comparison to dual-energy spectral CT[90].

**TABLE 2.**

Recommended imaging modalities for evaluation at each clinical stage of disease

| | Recommended imaging modality |
|---|---|
| Suspected renal mass | US, CT, MRI |
| Renal mass characterization | CT, MRI, US |
| RCC staging | CT, MRI |
| Restaging post-treatment | CT |
| Neurological symptoms | MRI, CT |
| Bone pain/increased alkaline phosphatase | Bone scintigraphy |

*CT: computed tomography; MRI: magnetic resonance imaging; RCC: renal cell carcinoma; US: ultrasound.*

Novel PET radiotracers linked to specific proteins, such as prostate-specific membrane antigen (PSMA) and carbonic anhydrase IX (CAIX), are under current investigation for the evaluation of RCC.

A systemic review showed that PSMA PET/CT has a potential role in staging, restaging, and predicting treatment response, but not for primary tumor evaluation[91]. It appears superior to FDG PET/CT for detection of local recurrence and bone metastases[92]. CAIX is a cell-surface antigen that is highly expressed in ccRCC but not found in other RCC subtypes or benign renal tissue (Figure 12). Girentuximab is an anti-CAIX monoclonal antibody. Preliminary studies showed that 89Zr-girentuximab PET/CT was able to differentiate between ccRCC and non-ccRCC[93], and improved detection of RCC metastases compared to CT alone or CT in combination with FDG PET/CT[94]. Theragnostic applications directed at PSMA and CAIX are being explored[95].

99m Technetium sestamibi is a radiotracer that accumulates in mitochondria-rich cells, and is commonly utilized in myocardial and parathyroid scintigraphy. Renal oncocytoma has high mitochondrial content compared to chRCC. A meta-analysis showed that 99m

**FIGURE 12.**

PET/CT targeting carbonic anhydrase IX in patient with metastatic clear cell renal cell carcinoma

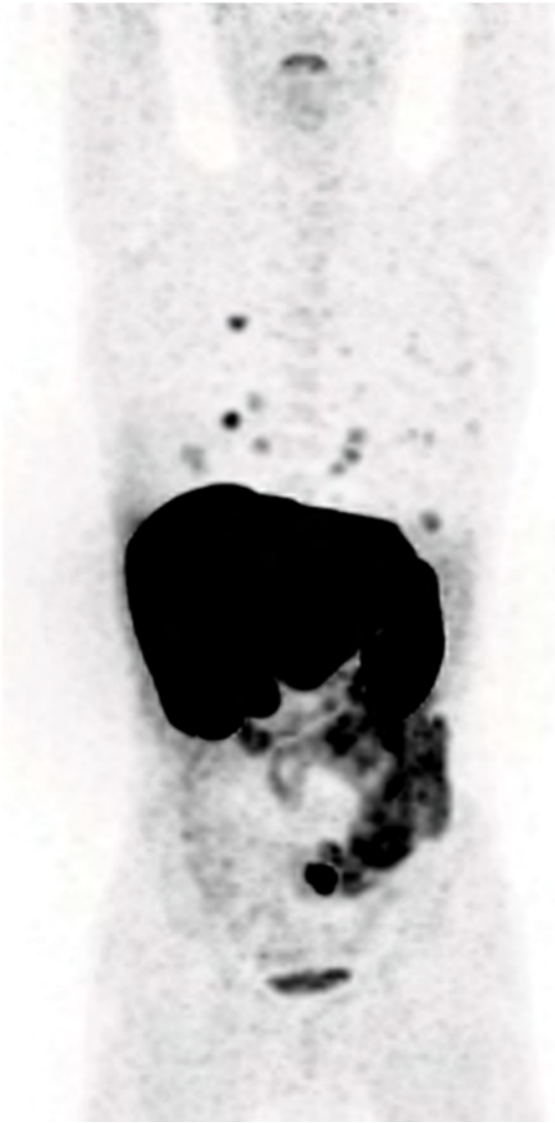

Maximum intensity projection image of 18F-VM4-037, a small molecule targeting carbonic anhydrase IX, in a patient with metastatic clear cell renal cell carcinoma. Physiologic soft palate, and hepatic, renal, gastrointestinal, and bladder activity is intense, while metastatic lung lesions are focal.

Technetium sestamibi scintigraphy had a pooled sensitivity and specificity of 92% and 88%, respectively, for detecting renal oncocytomas versus other renal lesions, and 89% and 67%, respectively, for detecting renal oncocytoma versus chRCC[96]. Novel application of this radiotracer to further characterize indeterminate renal masses would allow for triage of suspected oncocytomas to active surveillance.

Radiomics with artificial intelligence is an emerging field that uses computational methods to extract quantitative metrics, such as shape, size, and texture, from any standard clinical image dataset, such as CT, MRI or PET/CT, which can then be used to help differentiate between benign and malignant renal masses, predict nuclear grade, and evaluate gene expression profile[97]. Preliminary studies have shown that radiomics allows for differentiation of benign from malignant renal masses with CT[98,99] and MRI[100,101]. One CT study showed that sensitivity and accuracy were 85.8% and 74.4%, respectively, in differentiating ccRCC from oncocytoma[98]. Another CT study of 127 patients with RCC showed a sensitivity, specificity, and accuracy of 89%, 92%, and 87%, respectively, for differentiating ccRCC from non-ccRCC, and 87%, 92%, and 78%, respectively, for differentiating pRCC from chRCC[102]. A further CT study of 62 patients with pRCC showed 84% accuracy in differentiating between type 1 and type 2 pRCC[103]. An MRI study found a sensitivity, specificity, and accuracy of 92%, 41%, and 70%, respectively, for distinguishing benign from malignant renal masses when utilizing deep learning algorithms[100]. Studies have shown feasibility of radiomics to differentiate between low- and high-grade RCC[104,105]. One study of 53 patients showed a sensitivity, specificity, and accuracy of 91.3%, 80.6%, and 85.1%, respectively, for predicting high-grade from low-grade clear cell RCC[106].

Radiogenomic studies have shown that BRCA1-associated protein 1 mutation is associated with ill-defined tumor margins and presence of calcification, and more commonly seen with higher grade RCC[107]. Mutation of mucin 4 is found to be associated with exophytic tumor growth and reduced survival[107], while mutation of lysine demethylase 5C is found to be associated with renal vein invasion and reduced survival[108]. However, a systemic review of 57 studies found that translation of radiomics into clinical practice remains technically challenging owing to several factors including heterogeneous image acquisition protocols, reproducibility of radiomics signature, and big data sharing[109].

## Conclusion

Imaging plays a central role in the clinical detection, staging, and follow-up of patients with RCC. Contemporary management of RCC has emphasized the role of imaging in the multidisciplinary care of these patients. Clinicians should be cognizant of the strengths and limitations of the different imaging techniques. Newer imaging techniques and the nascent role of artificial intelligence may translate into future clinical practice.

## References


1. Moch H, Cubilla AL, Humphrey PA, Reuter VE, Ulbright TM. The 2016 WHO classification of tumours of the urinary system and male genital organs – Part A: renal, penile, and testicular tumours. *Eur Urol.*2016; 70:93-105. DOI:10.1016/j.eururo.2016.02.029.

2. Wang ZJ, Nikolaidis P, Khatri G, Dogra VS, Ganeshan D, Goldfarb S, et al. ACR appropriateness criteria® indeterminate renal mass. *J Am Coll Radiol.*2020; 17:S415-428. DOI:10.1016/j.jacr.2020.09.010.

3. Vogel C, Ziegelmuller B, Ljungberg B, Bensalah K, Bex A, Canfield S, et al. Imaging in suspected renal-cell carcinoma: systematic review. *Clin Genitourin Cancer.*2019; 17:e345-55. DOI:10.1016/j.clgc.2018.07.024.

4. Xue LY, Lu Q, Huang BJ, Ma JJ, Yan LX, Wen JX, et al. Contrast-enhanced ultrasonography for evaluation of cystic renal mass: in comparison to contrast-enhanced CT and conventional ultrasound. *Abdom Imaging.*2014; 39:1274-1283. DOI:10.1007/s00261-014-0171-4.

5. Park BK, Kim B, Kim SH, Ko K, Lee HM, Choi HY. Assessment of cystic renal masses based on Bosniak classification: comparison of CT and contrast-enhanced US. *Eur J Radiol.*2007;61:310-314. DOI:10.1016/j.ejrad.2006.10.004.

6. Cantisani V, Bertolotto M, Clevert DA, Correas JM, Drudi FM, Fischer T, et al. EFSUMB 2020 proposal for a contrast-enhanced ultrasound-adapted Bosniak cyst categorization – position statement. *Ultraschall Med.*2021;42:154-66. DOI:10.1055/a-1300-1727.

7. Campbell SC, Clark PE, Chang SS, Karam JA, Souter L, Uzzo RG. Renal mass and localized renal cancer: evaluation, management, and follow-up: AUA guideline: Part I. *J Urol.*2021;206:199-208. DOI:10.1097/JU.0000000000001911.

8. Ljungberg B, Albiges L, Abu-Ghanem Y, Bedke J, Capitanio U, Dabestani S, et al. European association of urology guidelines on renal cell carcinoma: the 2022 update. *Eur Urol.*2022; 25;S0302-2838(22)01676-1. DOI:10.1016/j.eururo.2022.03.006.

9. Motzer RJ, Jonasch E, Agarwal N, Alva A, Baine M, Beckermann K, et al. Kidney cancer, version 3.2022, NCCN clinical practice guidelines in oncology. *J Natl Compr Canc Netw.*2022;20:71-90. DOI:10.6004/jnccn.2022.0001.

10. Jena R, Narain TA, Singh UP, Srivastava A. Role of positron emission tomography/computed tomography in the evaluation of renal cell carcinoma. *Indian J Urol.*2021; 37:125-132. DOI:10.4103/iju.IJU_268_20.

11. Burgan CM, Sanyal R, Lockhart ME. Ultrasound of renal masses. *Radiol Clin North Am.*2019; 57:585-600. DOI:10.1016/j.rcl.2019.01.009.

12. Gulati M, King KG, Gill IS, Pham V, Grant E, Duddalwar VA. Contrast-enhanced ultrasound (CEUS) of cystic and solid renal lesions: a review. *Abdom Imaging.*2015;40:1982-1996. DOI:10.1007/s00261-015-0348-5.

13. King KG. Use of contrast ultrasound for renal mass evaluation. *Radiol Clin North Am.*2020; 58:935-949. DOI:10.1016/j.rcl.2020.05.002.

14. Sun MR, Ngo L, Genega EM, Atkins MB, Finn ME, Rofsky NM, et al. Renal cell carcinoma: dynamic contrast-enhanced MR imaging for differentiation of tumor subtypes – correlation with pathologic findings. *Radiology.*2009; 250:793-802. DOI:10.1148/radiol.2503080995.

15. Oliva MR, Glickman JN, Zou KH, Teo SY, Mortele KJ, Rocha MS, et al. Renal cell carcinoma: t1 and t2 signal intensity characteristics of papillary and clear cell types correlated with pathology. *AJR Am J Roentgenol.*2009; 192:1524-1530. DOI:10.2214/AJR.08.1727.

16. Eilenberg SS, Lee JK, Brown J, Mirowitz SA, Tartar VM. Renal masses: evaluation with gradient-echo Gd-DTPA-enhanced dynamic MR imaging. *Radiology.*1990; 176:333-338. DOI:10.1148/radiology.176.2.2367649.

17. Karlo CA, Donati OF, Burger IA, Zheng J, Moskowitz CS, Hricak H, et al. MR imaging of renal cortical tumours: qualitative and quantitative chemical shift imaging parameters. *Eur Radiol.*2013;23:1738-1744. DOI:10.1007/s00330-012-2758-x.

18. Tsili AC, Argyropoulou MI, Gousia A, Kalef-Ezra J, Sofikitis N, Malamou-Mitsi V, et al. Renal cell carcinoma: value of multiphase MDCT with multiplanar reformations in the detection of pseudocapsule. *AJR Am J Roentgenol.*2012; 199:379-386. DOI:10.2214/AJR.11.7747.

19. Roy C, El Ghali S, Buy X, Lindner V, Lang H, Saussine C, et al. Significance of the pseudocapsule on MRI of renal neoplasms and its potential application for local staging: a retrospective study. *AJR Am J Roentgenol.*2005;184:113-120. DOI:10.2214/ajr.184.1.01840113.

20. Kim JK, Kim TK, Ahn HJ, Kim CS, Kim KR, Cho KS. Differentiation of subtypes of renal cell carcinoma on helical CT scans. *AJR Am J Roentgenol.*2002; 178:1499-1506. DOI:10.2214/ajr.178.6.1781499.

21. Couvidat C, Eiss D, Verkarre V, Merran S, Correas JM, Mejean A, et al. Renal papillary carcinoma: CT and MRI features. *Diagn Interv Imaging.*2014; 95:1055-1063. DOI:10.1016/j.diii.2014.03.013.

22. Yoshimitsu K, Kakihara D, Irie H, Tajima T, Nishie A, Asayama Y, et al. Papillary renal carcinoma: diagnostic approach by chemical shift gradient-echo and echo-planar MR imaging. *J Magn Reson Imaging.*2006;23:339-344. DOI:10.1002/jmri.20509.

23. Pedrosa I, Sun MR, Spencer M, Genega EM, Olumi AF, Dewolf WC, et al. MR imaging of renal masses: correlation with findings at surgery and pathologic analysis. *Radiographics.*2008; 28:985-1003. DOI:10.1148/rg.284065018.

24. Egbert ND, Caoili EM, Cohan RH, Davenport MS, Francis IR, Kunju LP, et al. Differentiation of papillary renal cell carcinoma subtypes on CT and MRI. *AJR Am J Roentgenol.*2013;201:347-355. DOI:10.2214/AJR.12.9451.

25. Rosenkrantz AB, Hindman N, Fitzgerald EF, Niver BE, Melamed J, Babb JS. MRI features of renal oncocytoma and chromophobe renal cell carcinoma. *AJR Am J Roentgenol.*2010;195:W421-7. DOI:10.2214/AJR.10.4718.

26. Raman SP, Johnson PT, Allaf ME, Netto G, Fishman EK. Chromophobe renal cell carcinoma: multiphase MDCT enhancement patterns and morphologic features. *AJR Am J Roentgenol*.2013; 201:1268-1276. DOI:10.2214/AJR.13.10813.

27. Wu J, Zhu Q, Zhu W, Chen W, Wang S. Comparative study of CT appearances in renal oncocytoma and chromophobe renal cell carcinoma. *Acta Radio*l.2016; 57:500-506. DOI:10.1177/0284185115585035.

28. Monn MF, Gellhaus PT, Patel AA, Masterson TA, Tann M, Boris RS. Can radiologists and urologists reliably determine renal mass histology using standard preoperative computed tomography imaging? *J Endourol*.2015;29:391-396. DOI:10.1089/end.2014.0560.

29. Lesavre A, Correas JM, Merran S, Grenier N, Vieillefond A, Helenon O. CT of papillary renal cell carcinomas with cholesterol necrosis mimicking angiomyolipomas. *AJR Am J Roentgenol*.2003; 181:143-145. DOI:10.2214/ajr.181.1.1810143.

30. Hindman N, Ngo L, Genega EM, Melamed J, Wei J, Braza JM, et al. Angiomyolipoma with minimal fat: can it be differentiated from clear cell renal cell carcinoma by using standard MR techniques? *Radiology*.2012; 265:468-477. DOI:10.1148/radiol.12112087.

31. Dilauro M, Quon M, McInnes MD, Vakili M, Chung A, Flood TA, et al. Comparison of contrast-enhanced multiphase renal protocol CT versus MRI for diagnosis of papillary renal cell carcinoma. *AJR Am J Roentgenol*.2016;206:319-325. DOI:10.2214/AJR.15.14932.

32. Sasiwimonphan K, Takahashi N, Leibovich BC, Carter RE, Atwell TD, Kawashima A. Small (<4cm) renal mass: differentiation of angiomyolipoma without visible fat from renal cell carcinoma utilizing MR imaging. *Radiology*.2012;263:160-168. DOI:10.1148/radiol.12111205.

33. Galmiche C, Bernhard JC, Yacoub M, Ravaud A, Grenier N, Cornelis F. Is multiparametric MRI useful for differentiating oncocytomas from chromophobe renal cell carcinomas? *AJR Am J Roentgenol*.2017;208:343-350. DOI:10.2214/AJR.16.16832.

34. Lee-Felker SA, Felker ER, Tan N, Margolis DJA, Young JR, Sayre J, et al. Qualitative and quantitative MDCT features for differentiating clear cell renal cell carcinoma from other solid renal cortical masses. *AJR Am J Roentgenol*.2014;203:W516-24. DOI:10.2214/AJR.14.12460.

35. Young JR, Coy H, Kim HJ, Douek M, Lo P, Pantuck AJ, et al. Performance of relative enhancement on multiphasic MRI for the differentiation of clear cell renal cell carcinoma (RCC) from papillary and chromophobe RCC subtypes and oncocytoma. *AJR Am J Roentgenol*.2017;208:812-819. DOI:10.2214/AJR.16.17152.

36. Kang SK, Zhang A, Pandharipande PV, Chandarana H, Braithwaite RS, Littenberg B. DWI for renal mass characterization: systematic review and meta-analysis of diagnostic test performance. *AJR Am J Roentgenol*.2015;205:317-324. DOI:10.2214/AJR.14.13930.

37. Yan L, Liu Z, Wang G, Huang Y, Liu Y, Yu Y, et al. Angiomyolipoma with minimal fat: differentiation from clear cell carcinoma by texture analysis on CT images. *Acad Radiol*.2015; 22:1115-1121. DOI:10.1016/j.acra.2015.04.004.

38. Kay FU, Canvasser NE, Xi Y, Pinho DF, Costa DN, Diaz de Leon A, et al. Diagnostic performance and interreader agreement of a standardized MR imaging approach in the prediction of small renal mass histology. *Radiology*.2018;287:543-553. DOI:10.1148/radiol.2018171557.

39. Roussel E, Capitanio U, Kutikov A, Oosterwijk E, Pedrosa I, Rowe SP, et al. Novel imaging methods for renal mass characterization: a collaborative review. *Eur Urol*.2022;81:476-488. DOI:10.1016/j.eururo.2022.01.040.

40. Hou G, Zhao D, Jiang Y, Zhu Z, Huo L, Li F, et al. Clinical utility of FDG PET/CT for primary and recurrent papillary renal cell carcinoma. *Cancer Imaging*.2021;21:25. DOI:10.1186/s40644-021-00393-8.

41. Nikpanah M, Paschall AK, Ahlman MA, Civelek AC, Farhadi F, Mirmomen SM, et al. 18Fluorodeoxyglucose-positron emission tomography/computed tomography for differentiation of renal tumors in hereditary kidney cancer syndromes. *Abdom Radiol (NY)*.2021;46:3301-3308. DOI:10.1007/s00261-021-02999-9.

42. Nakajima R, Abe K, Kondo T, Tanabe K, Sakai S. Clinical role of early dynamic FDG-PET/CT for the evaluation of renal cell carcinoma. *Eur Radiol*.2016; 26:1852-1862. DOI:10.1007/s00330-015-4026-3.

43. Nakajima R, Nozaki S, Kondo T, Nagashima Y, Abe K, Sakai S. Evaluation of renal cell carcinoma histological subtype and Fuhrman grade using 18F-fluorodeoxyglucose-positron emission tomography/computed tomography. *Eur Radiol*.2017;27:4866-4873. DOI:10.1007/s00330-017-4875-z.

44. Ficarra V, Righetti R, Martignoni G, D'Amico A, Pilloni S, Rubilotta E, et al. Prognostic value of renal cell carcinoma nuclear grading: multivariate analysis of 333 cases. *Urol Int*.2001;67:130-134. DOI:10.1159/000050968.

45. Pedrosa I, Chou MT, Ngo L, Baroni RH, Genega EM, Galaburda L, et al. MR classification of renal masses with pathologic correlation. *Eur Radiol*.2008;18:365-375. DOI:10.1007/s00330-007-0757-0.

46. Cornelis F, Tricaud E, Lasserre AS, Petitpierre F, Bernhard JC, Le Bras Y, et al. Multiparametric magnetic resonance imaging for the differentiation of low and high grade clear cell renal carcinoma. *Eur Radiol*.2015;25:24-31. DOI:10.1007/s00330-014-3380-x.

47. Schieda N, Thornhill RE, Al-Subhi M, McInnes MD, Shabana WM, van der Pol CB, et al. Diagnosis of sarcomatoid renal cell carcinoma with CT: evaluation by qualitative imaging features and texture analysis. *AJR Am J Roentgenol*.2015;204:1013-1023. DOI:10.2214/AJR.14.13279.

48. Young JR, Young JA, Margolis DJA, Sauk S, Sayre J, Pantuck AJ, et al. Sarcomatoid renal cell carcinoma and collecting duct carcinoma: discrimination from common renal cell carcinoma subtypes and benign RCC mimics on multiphasic MDCT. *Acad Radiol*.2017;24:1226-32. DOI:10.1016/j.acra.2017.03.017.

49. Hindman NM, Bosniak MA, Rosenkrantz AB, Lee-Felker S, Melamed J. Multilocular cystic renal cell carcinoma: comparison of imaging and pathologic findings. *AJR Am J Roentgenol*.2012;198:W20-26. DOI:10.2214/AJR.11.6762.

50. Zhu H, Zhao S, Zuo C, Ren F. FDG PET/CT and CT findings of renal cell carcinoma with sarcomatoid differentiation. *AJR Am J Roentgenol*.2020;215:645-651. DOI:10.2214/AJR.19.22467.

51. Singh H, Arora G, Nayak B, Sharma A, Singh G, Kumari K, et al. Semi-quantitative F-18-FDG PET/computed tomography parameters for prediction of grade in patients with renal cell carcinoma and the incremental value of diuretics. *Nucl Med Commun.*2020;41:485-493. DOI:10.1097/MNM.0000000000001169.

52. Zhao Y, Wu C, Li W, Chen X, Li Z, Liao X, et al. 2-[18F]FDG PET/CT parameters associated with WHO/ISUP grade in clear cell renal cell carcinoma. *Eur J Nucl Med Mol Imaging.*2021;48:570-579. DOI:10.1007/s00259-020-04996-4.

53. Coy H, Young JR, Pantuck AJ, Douek ML, Sisk A, Magyar C, et al. Association of tumor grade, enhancement on multiphasic CT and microvessel density in patients with clear cell renal cell carcinoma. *Abdom Radiol (NY).*2020;45:3184-3192. DOI:10.1007/s00261-019-02271-1.

54. Woo S, Suh CH, Kim SY, Cho JY, Kim SH. Diagnostic performance of DWI for differentiating high- from low-grade clear cell renal cell carcinoma: a systematic review and meta-analysis. *AJR Am J Roentgenol.*2017;209:W374-381. DOI:10.2214/AJR.17.18283.

55. Cui E, Li Z, Ma C, Li Q, Lei Y, Lan Y, et al. Predicting the ISUP grade of clear cell renal cell carcinoma with multiparametric MR and multiphase CT radiomics. *Eur Radiol.*2020;30:2912-2921. DOI:10.1007/s00330-019-06601-1.

56. Zhang L, Zhao H, Jiang H, Zhao H, Han W, Wang M, et al. 18F-FDG texture analysis predicts the pathological Fuhrman nuclear grade of clear cell renal cell carcinoma. *Abdom Radiol (NY).*2021;46:5618-5628. DOI:10.1007/s00261-021-03246-x.

57. Amin MB, Edge SB. AJCC Cancer staging manual, 8th Edition. *Springer Nature Switzerland AG*; 2017.

58. Vikram R, Beland MD, Blaufox MD, Moreno CC, Gore JL, Harvin HJ, et al. ACR appropriateness criteria renal cell carcinoma staging. *J Am Coll Radiol.*2016;13:518-525. DOI:10.1016/j.jacr.2016.01.021.

59. Hallscheidt PJ, Bock M, Riedasch G, Zuna I, Schoenberg SO, Autschbach F, et al. Diagnostic accuracy of staging renal cell carcinomas using multidetector-row computed tomography and magnetic resonance imaging: a prospective study with histopathologic correlation. *J Comput Assist Tomogr.*2004;28:333-339. DOI:10.1097/00004728-200405000-00005.

60. Walter C, Kruessell M, Gindele A, Brochhagen HG, Gossmann A, Landwehr P. Imaging of renal lesions: evaluation of fast MRI and helical CT. *Br J Radiol.*2003;76:696-703. DOI:10.1259/bjr/33169417.

61. Campbell SC, Uzzo RG, Karam JA, Chang SS, Clark PE, Souter L. Renal mass and localized renal cancer: evaluation, management, and follow-up: AUA guideline: Part II. *J Urol.*2021;206:209-218. DOI:10.1097/JU.0000000000001912.

62. Gerety EL, Lawrence EM, Wason J, Yan H, Hilborne S, Buscombe J, et al. Prospective study evaluating the relative sensitivity of 18F-NaF PET/CT for detecting skeletal metastases from renal cell carcinoma in comparison to multidetector CT and 99mTc-MDP bone scintigraphy, using an adaptive trial design. *Ann Oncol.*2015;26:2113-8. DOI:10.1093/annonc/mdv289.

63. Elkassem AA, Allen BC, Sharbidre KG, Rais-Bahrami S, Smith AD. Update on the role of imaging in clinical staging and restaging of renal cell carcinoma based on the AJCC 8th edition, from the AJR special series on cancer staging. *AJR Am J Roentgenol.*2021;217:541-555. DOI:10.2214/AJR.21.25493.

64. Jeffrey NN, Douek N, Guo DY, Patel MI. Discrepancy between radiological and pathological size of renal masses. *BMC Urol.*2011;11:2. DOI:10.1186/1471-2490-11-2.

65. Bolster F, Durcan L, Barrett C, Lawler LP, Cronin CG. Renal cell carcinoma; accuracy of multidetector computed tomography in the assessment of renal sinus fat invasion. *J Comput Assist Tomogr.*2016;40:851-855. DOI:10.1097/RCT.0000000000000448.

66. Takamatsu A, Yoshida K, Obokata M, Inoue D, Yoneda N, Kadono Y, et al. Urinary collecting system invasion on multiphasic CT in renal cell carcinomas: prevalence, characteristics, and clinical significance. *Abdom Radiol (NY).*2021;46:2090-2096. DOI:10.1007/s00261-020-02859-y.

67. Hedgire SS, Elmi A, Nadkarni ND, Cao K, McDermott S, Harisinghani MG. Preoperative evaluation of perinephric fat invasion in patients with renal cell carcinoma: correlation with pathological findings. *Clin Imaging.*2013;37:91-96. DOI:10.1016/j.clinimag.2012.03.005.

68. Bianchi M, Sun M, Jeldres C, Shariat SF, Trinh QD, Briganti A, et al. Distribution of metastatic sites in renal cell carcinoma: a population-based analysis. *Ann Oncol.*2012;23:973-980. DOI:10.1093/annonc/mdr362.

69. Griffin N, Gore ME, Sohaib SA. Imaging in metastatic renal cell carcinoma. *AJR Am J Roentgenol.*2007;189:360-370. DOI:10.2214/AJR.07.2077.

70. Heidenreich A, Ravery V, European Society of Oncological Urology. Preoperative imaging in renal cell cancer. *World J Urol.*2004;22:307-315. DOI:10.1007/s00345-004-0411-2.

71. Tadayoni A, Paschall AK, Malayeri AA. Assessing lymph node status in patients with kidney cancer. *Transl Androl Urol.*2018;7:766-773. DOI:10.21037/tau.2018.07.19.

72. Ljungberg B, Alamdari FI, Rasmuson T, Roos G. Follow-up guidelines for nonmetastatic renal cell carcinoma based on the occurrence of metastases after radical nephrectomy. *BJU Int.*1999;84:405-411. DOI:10.1046/j.1464-410x.

73. Rossi SH, Prezzi D, Kelly-Morland C, Goh V. Imaging for the diagnosis and response assessment of renal tumours. *World J Urol.*2018;36:1927-1942. DOI:10.1007/s00345-018-2342-3.

74. Ma H, Shen G, Liu B, Yang Y, Ren P, Kuang A. Diagnostic performance of 18F-FDG PET or PET/CT in restaging renal cell carcinoma: a systemic review and meta-analysis. *Nucl Med Commun.*2017;38:156-163. DOI:10.1097/MNM.0000000000000618.

75. Park S, Lee HY, Lee S. Role of F-18 FDG PET/CT in the follow-up of asymptomatic renal cell carcinoma patients for postoperative surveillance: based on conditional survival analysis. *J Cancer Res Clin Oncol.2022;*148:215-224. DOI:10.1007/s00432-021-03688-2.

76. Alongi P, Picchio M, Zattoni F, Spallino M, Gianolli L, Saladini G, et al. Recurrent renal cell carcinoma: clinical and prognostic value of FDG PET/CT. *Eur J Nucl Med Mol Imaging.*2016;43:464-473. DOI:10.1007/s00259-015-3159-6.

77. Kayani I, Avril N, Bomanji J, Chowdhury S, Rockall A, Sahdev A, et al. Sequential FDG-PET/CT as a biomarker of response to sunitinib in metastatic clear cell renal cancer. *Clin Cancer Res.*2011;17:6021-6028. DOI:10.1158/1078-0432.CCR-10-3309.

78. Minamimoto R, Barkhodari A, Harshman L, Srinivas S, Quon A. Prognostic value of quantitative metabolic metrics on baseline pre-sunitinib FDG PET/CT in advanced renal cell carcinoma. *PLoS One.*2016;11:e0153321. DOI:10.1371/journal.pone.0153321.

79. Hwang SH, Cho A, Yun M, Choi YD, Rha SY, Kang WJ. Prognostic value of pretreatment metabolic tumor volume and total lesion glycolysis using 18F-FDG PET/CT in patients with metastatic renal cell carcinoma treated with anti-vascular endothelial growth factor-targeted agents. *Clin Nucl Med.*2017;42:e235-241. DOI:10.1097/RLU.0000000000001612.

80. Bhosale PR, Wei W, Ernst RD, Bathala TK, Reading RM, Wood CG, et al. Intraoperative sonography during open partial nephrectomy for renal cell cancer: does it alter surgical management? *AJR Am J Roentgenol.*2014;203:822-827. DOI:10.2214/AJR.13.12254.

81. Li Q, Li N, Luo Y, Yu H, Ma X, Zhang X, et al. Role of intraoperative ultrasound in robotic-assisted radical nephrectomy with inferior vena cava thrombectomy in renal cell carcinoma. *World J Urol.*2020;38:3191-3198. DOI:10.1007/s00345-020-03141-y.

82. Wake N, Bjurlin MA, Rostami P, Chandarana H, Huang WC. Three-dimensional printing and augmented reality: enhanced precision for robotic assisted partial nephrectomy. *Urology.*2018;116:227-228. DOI:10.1016/j.urology.2017.12.038.

83. Bernhard JC, Isotani S, Matsugasumi T, Duddalwar V, Hung AJ, Suer E, et al. Personalized 3D printed model of kidney and tumor anatomy: a useful tool for patient education. *World J Urol.*2016;34:337-345. DOI:10.1007/s00345-015-1632-2.

84. Campi R, Stewart GD, Staehler M, Dabestani S, Kuczyk MA, Shuch BM, et al. Novel liquid biomarkers and innovative imaging for kidney cancer diagnosis: what can be implemented in our practice today? A systematic review of the literature. *Eur Urol Oncol.*2021;4:22-41. DOI:10.1016/j.euo.2020.12.011.

85. Roussel E, Capitanio U, Kutikov A, Oosterwijk E, Pedrosa I, Rowe SP, et al. Novel imaging methods for renal mass characterization: a collaborative review. *Eur Urol.*2022;81:476-488. DOI:10.1016/j.eururo.2022.01.040.

86. Sagreiya H, Akhbardeh A, Li D, Sigrist R, Chung BI, Sonn GA, et al. Point shear wave elastography using machine learning to differentiate renal cell carcinoma and angiomyolipoma. *Ultrasound Med Biol.*2019;45:1944-1954. DOI:10.1016/j.ultrasmedbio.2019.04.009.

87. Chen C, Kang Q, Xu B, Shi Z, Guo H, Wei Q, et al. Fat poor angiomyolipoma differentiation from renal cell carcinoma at 320-slice dynamic volume CT perfusion. *Abdom Radiol (NY).*2018;43:1223-1230. DOI:10.1007/s00261-017-1286-1.

88. Wang D, Huang X, Bai L, Zhang X, Wei J, Zhou J. Differential diagnosis of chromophobe renal cell carcinoma and papillary renal cell carcinoma with dual-energy spectral computed tomography. *Acta Radiol.*2020;61:1562-1569. DOI:10.1177/0284185120903447.

89. Wei J, Zhao J, Zhang X, Wang D, Zhang W, Wang Z, et al. Analysis of dual energy spectral CT and pathological grading of clear cell renal cell carcinoma (ccRCC). *PLoS One.*2018;13:e0195699. DOI:10.1371/journal.pone.0195699.

90. Manoharan D, Netaji A, Diwan K, Sharma S. Normalized dual-energy iodine ratio best differentiates renal cell carcinoma subtypes among quantitative imaging biomarkers from perfusion CT and dual-energy CT. *AJR Am J Roentgenol.*2020;215:1389-1397. DOI:10.2214/AJR.19.22612.

91. Van de Wiele C, Sathekge M, de Spiegeleer B, de Jonghe PJ, Beels L, Maes A. PSMA-targeting positron emission agents for imaging solid tumors other than non-prostate carcinoma: a systematic review. *Int J Mol Sci.*2019;20:4886. DOI:10.3390/ijms20194886.

92. Liu Y, Wang G, Yu H, Wu Y, Lin M, Gao J, et al. Comparison of 18F-DCFPyL and 18F-FDG PET/computed tomography for the restaging of clear cell carcinoma: preliminary results of 15 patients. *Nucl Med Commun.*2020;41:1299-12305. DOI:10.1097/MNM.0000000000001285.

93. Merkx RIJ, Lobeek D, Konijnenberg M, Jimenez-Franco LD, Kluge A, Oosterwijk E, et al. Phase I study to assess safety, biodistribution and radiation dosimetry for 89Zr-girentuximab in patients with renal cell carcinoma. *Eur J Nucl Med Mol Imaging.*2021;48:3277-3285. DOI:10.1007/s00259-021-05271-w.

94. Verhoeff SR, van Es SC, Boon E, van Helden E, Angus L, Elias SG, et al. Lesion detection by [89Zr]Zr-DFO-girentuximab and [18F]FDG-PET/CT in patients with newly diagnosed metastatic renal cell carcinoma. *Eur J Nucl Med Mol Imaging.*2019;46:1931-1939. DOI:10.1007/s00259-019-04358-9.

95. Muselaers CHJ, Boers-Sonderen MJ, van Oostenbrugge TJ, Boerman OC, Desar IME, Stillebroer AB, et al. Phase 2 study of lutetium 177-labeled anti-carbonic anhydrase IX monoclonal antibody girentuximab in patients with advanced renal cell carcinoma. *Eur Urol.*2016;69:767-770. DOI:10.1016/j.eururo.2015.11.033.

96. Wilson MP, Katlariwala P, Murad MH, Abele J, McInnes MDF, Low G. Diagnostic accuracy of 99mTc-sestamibi SPECT/CT for detecting renal oncocytomas and other benign renal lesions: a systematic review and meta-analysis. *Abdom Radiol (NY).*2020;45:2532-2541. DOI:10.1007/s00261-020-02469-8.

97. Suarez-Ibarrola R, Hein S, Reis G, Gratzke C, Miernik A. Current and future applications of machine and deep learning in urology: a review of the literature on urolithiasis, renal cell carcinoma, and bladder and prostate cancer. *World J Urol.*2020;38:2329-2347. DOI:10.1007/s00345-019-03000-5.

98. Coy H, Hsieh K, Wu W, Nagarajan MB, Young JR, Douek ML, et al. Deep learning and radiomics: the utility of Google TensorFlowTM Inception in classifying clear cell renal cell carcinoma and oncocytoma on multiphasic CT. *Abdom Radiol (NY).*2019;44:2009-2020. DOI:10.1007/s00261-019-01929-0.

99. Yap FY, Varghese BA, Cen SY, Hwang DH, Lei X, Desai B, et al. Shape and texture-based radiomics signature on CT effectively discriminates benign from malignant renal masses. *Eur Radiol.*2021;31:1011-1021. DOI:10.1007/s00330-020-07158-0.

100. Xi IL, Zhao Y, Wang R, Chang M, Purkayastha S, Chang K, et al. Deep learning to distinguish benign from malignant renal lesions based on routine MR imaging. *Clin Cancer Res.*2020;26:1944-1952. DOI:10.1158/1078-0432.CCR-19-0374.

101. Vendrami CL, McCarthy RJ, Villavicencio CP, Miller FH. Predicting common solid renal tumors using machine learning models of classification of radiologist-assessed magnetic resonance characteristics. A*bdom Radiol (NY).*2020;45:2797-2809. DOI:10.1007/s00261-020-02637-w.

102. Zhang GMY, Shi B, Xue HD, Ganeshan B, Sun H, Jin ZY. Can quantitative CT texture analysis be used to differentiate subtypes of renal cell carcinoma? *Clin Radiol.*2019;74:287-294. DOI:10.1016/j.crad.2018.11.009.

103. Duan C, Li N, Niu L, Wang G, Zhao J, Liu F, et al. CT texture analysis for the differentiation of papillary renal cell carcinoma subtypes. *Abdom Radiol (NY).*2020;45:3860-3868. DOI:10.1007/s00261-020-02588-2.

104. Huhdanpaa H, Hwang D, Cen S, Quinn B, Nayyar M, Zhang X, et al. CT prediction of the Fuhrman grade of clear cell renal cell carcinoma (RCC): towards the development of computer-assisted diagnostic method. *Abdom Imaging.*2015;40:3168-174. DOI:10.1007/s00261-015-0531-8.

105. Shu J, Wen D, Xi Y, Xia Y, Cai Z, Xu W, et al. Clear cell renal cell carcinoma: machine learning-based computed tomography radiomics analysis for the prediction of WHO/ISUP grade. *Eur J Radiol.*2019;121:108738. DOI:10.1016/j.ejrad.2019.108738.

106. Bektas CT, Kocak B, Yardimci AH, Turkcanoglu MH, Yucetas U, Koca SB, et al. Clear cell renal cell carcinoma: machine learning-based quantitative computed tomography texture analysis for prediction of Fuhrman nuclear grade. *Eur Radiol.*2019;29:1153-1163. DOI:10.1007/s00330-018-5698-2.

107. Shinagare AB, Vikram R, Jaffe C, Akin O, Kirby J, Huang E, et al. Radiogenomics of clear cell renal cell carcinoma: preliminary findings of the cancer genome atlas-renal cell carcinoma (TCGA-RCC) imaging research group. *Abdom Imaging.*2015;40:1684-1692. DOI:10.1007/s00261-015-0386-z.

108. Karlo CA, Di Paolo PL, Chaim J, Hakimi AA, Ostrovnaya I, Russo P, et al. Radiogenomics of clear cell carcinoma: associations between CT imaging features and mutations. *Radiology.*2014;270:464-471. DOI:10.1148/radiol.13130663.

109. Ursprung S, Beer L, Bruining A, Woitek R, Stewart GD, Gallagher FA, et al. Radiomics of computed tomography and magnetic resonance imaging in renal cell carcinoma – a systematic review and meta-analysis. *Eur Radiol.*2020;30:3558-3566. DOI:10.1007/s00330-020-06666-3.